Physics – Uspekhi **66** (9) 914 – 930 (2023)

REVIEWS OF TOPICAL PROBLEMS PACS numbers: 92.70.Gt, 92.70.Np, 92.70.Qr

Problems of parameterization of the radiation block in physical and mathematical climate models and the possibility of their solution

V M Fedorov

DOI: https://doi.org/10.3367/UFNe.2023.03.039339

Contents

Abstract. The problems associated with the failure to take into account periodic long-term and interannual changes in incoming solar radiation by latitudes and seasons, as well as long-term changes in the intensity of radiative heat transfer in the parameterization of the radiation block of physical and mathematical climate models, are shown. Existing problems with the radiation block parameterization limit the possibilities of modeling climate and forecasting its changes. To solve the problems, a review of Earth's insolation data with different time resolutions available for parameterization is presented.

Keywords: insolation, incoming solar radiation, secular and periodic fluctuations, interannual changes, radiative heat transfer, mathematical modeling, radiation block

1. Introduction

Climate is the most important characteristic of the human natural environment, so the study of global climate change is one of the most important scientific and practical challenges. Its relevance is determined by the demand for predicting the consequences of climate change for the natural environment, humans, and society. The most important issue in solving this problem is clarifying the causes of these changes [1–3]. Among the possible factors of climate formation and change, solar radiation, the greenhouse effect, volcanic activity, and heat exchange mechanisms are considered to be the basic ones.

Solar radiation is the main source of energy that determines the radiation and heat balance of Earth, its surface, and its atmosphere [4, 5]. The zonal arrangement of climatic regions is associated with the latitudinal features of the distribution of solar radiation. Altitudinal zonality is associated with a change in the amount of radiative heat with height. The change in the solar radiation arriving at the upper boundary of the atmosphere (UBA) is determined by two factors that have different physical natures. One of them is related to the change in the activity of the Sun. The other is determined by celestial-mechanical processes that change the elements of Earth's orbit: the Earth–Sun distance, the duration of the tropical year, etc., as well as the tilt of the axis of rotation and related changes in the daily, seasonal, and long-term solar radiation delivery, and its distribution over latitudes and seasons (solar climate of Earth). The solar (mathematical) climate is understood as the theoretically calculated supply and distribution of solar energy on the UBA or on Earth's surface in the absence of an atmosphere [6–9]. Thus, the UBA is starting point for the short-wave radiation coming to Earth and the radiation balance of Earth, its surface, and its atmosphere.

The redistribution of radiative heat in the atmosphere and ocean is associated with heat transfer mechanisms. The main ones are interlatitudinal heat transfer — meridional transfer of radiative heat from the equatorial region to the polar regions ('heat engine of the first kind'); heat exchange in the ocean–continent system, associated with seasonal change in the areas of heat source and sink ('heat engine of the second kind') [10]; heat transfer in the ocean–atmosphere system; interhemispheric heat transfer [11]; etc. An important factor in regulating Earth's thermal regime is the composition of the atmosphere (primarily the content of water vapor), which determines the value of the albedo — reflection of short-wave radiation coming from the Sun, the role of the greenhouse effect of the planet, and its change [12]. The intensity of radiative heat transfer is mainly associated with changes in Earth's solar climate, determined by astronomical factors [7, 13, 14]. In this regard, the content of the radiation block has priority, the basic value in the architecture of all climate models, since it reflects the main external energy signal

V M Fedorov
Lomonosov Moscow State University,
Leninskie gory, 119991 Moscow, Russian Federation
E-mail: fedorov.msu@mail.ru

Received 19 September 2022, revised 18 March 2023
Uspekhi Fizicheskikh Nauk **193** (9) 971 – 988 (2023)
Translated by V L Derbov

incoming to the simulated natural system and its components. Nevertheless, the existing problems of parameterizing the radiation block in the analysis of existing problems in climate modeling are not currently considered [15, 16].

Physical and mathematical climate models are a high-tech and necessary toolkit for scientific research. The need for modeling climatic processes is determined by the following: first, the heterogeneity of the components of the natural system (which is characterized by climate); second, the complexity and variety of connections among the components of the system (direct and reverse); third, a permanent variation in the state of both individual components and the natural system as a whole in space and time; fourth, the temporal and spatial variability of connections between the components of the natural system. Given the need and importance of modeling natural processes, improving or creating fundamentally new climate models (related to high technology) seems to be an urgent problem in natural science [17, 18]. Improving models is based on identifying problems in modeling and solving them. The aim of the present paper is to reveal the current problems in climate modeling related to the radiation block imperfection due to the limited reflection of the external energy signal entering the simulated system and to review the data that could be used to solve them.

2. Available radiative data (external energy signal)

2.1 Data reflecting solar activity variation

In the CMIP-51IPCC (Intergovernmental Panel on Climate Change) project, it is recommended to use the data [19, 20] obtained as a result of radiometric measurements of the total radiation flux (since 1978) and the total solar irradiance (TSI) reconstruction (since 1610 with annual resolution and since 1882 with monthly resolution) [21]. The total radiation flux reconstruction was based on solar activity variations (sunspots and flares). The Coupled Model Intercomparison Project (CMIP) is an international project to reproduce the current climate and predict its changes using coupled atmospheric and ocean models.

In the CMIP-6 project [22], in the radiation block of physical and mathematical climate models, it is recommended that the TSI reconstruction (for a period up to 9400 in the past) performed by F Steinhilber et al. be used [23]. The reconstruction was based on radionuclide records of Be^{10} content in ice cores from Greenland and Antarctica and C^{14} content in tree remains. Recall that TSI is understood as the total flux of solar radiation passing per unit time through a unit area oriented perpendicular to the flux at a distance of 1 astronomical unit (AU) from the Sun outside Earth's atmosphere. The transition from the value of solar radiation obtained for Earth's disk, located perpendicular to the Sun's rays at a distance of 1 AU from the Sun, to the value for the UBA of Earth is made by dividing this value by 4, since the area of the sphere is 4 times the area of its great circle. Thus, TSI is calculated for a sphere, despite the fact that Earth has the shape of an ellipsoid [1, 7, 8, 13].

It should be noted that these recommendations reflect the possibility of taking into account variations associated only with changes in solar activity. Naturally, they do not reflect changes in the total solar radiation flux, since they do not take into account variations associated with celestial-mechanical processes. Studies of variations in solar radiation associated with changes in the physical activity of the Sun have a long history (study of sunspots, Schwabe–Wolf, Hale, and Gleissberg cycles in the variation in solar activity). At the same time, the question of whether there is a relationship between changes in solar activity and climate has been debatable for a long time [24–28].

2.2 Data on Earth's insolation (solar climate)

2.2.1 Low-frequency (secular) variations in insolation. Consideration of variations in solar radiation associated with celestial-mechanical processes in the radiation block of physical-mathematical models can be (and is carried out in most models) based on theoretically calculated data on Earth's insolation (solar or mathematical climate). Such data were first obtained by the Serbian mathematician Milutin Milankovich. It should be noted that, since the purpose of his calculations was to explain the causes of glacial epochs in the Pleistocene, the calculations were performed with low spatial and temporal resolution [6, 29]. In addition, instead of calculating the sums of radiative heat for the summer and winter half-years, M Milankovich used caloric half-years, defined as half-years of the same duration ($T_0/2$) when, at a given latitude, any value of daily insolation in the summer half-year is greater than any value of daily insolation in the winter half-year (we note right away that this approach does not allow calculating the intensity of interhemispheric heat transfer). The duration of the tropical year — the period between two successive positions of Earth at the vernal equinox — was considered constant (which does not allow taking into account small variations in Earth's solar climate associated with the perturbed rather than Keplerian motion of Earth in orbit). Milankovich calculated insolation variations for eight parallels located between 5° and 75° north latitude. The main results of his research are presented in the book, *Mathematical climatology and the astronomical theory of climate change*, published in 1939 in Russian.

The calculations made by Milankovich were subsequently carried out and refined by a number of authors (Figs 1, 2). These calculations were based on new solutions to the theory of secular perturbations obtained for the entire solar system in 1950 by D Brouwer and A Van Woerkom [30]. The calculations used the latest data on the masses and motions of the planets, taking into account second-order effects caused, for example, by long-period variations in the motions of Jupiter and Saturn.

Detailed calculations of the solar radiation coming to the upper boundary of the atmosphere were carried out by the Soviet astronomers Sh G Sharaf and N A Budnikova [31]. They discovered errors in the original values of the longitudes of the nodes of Venus and Earth, used by D Brouwer and A Van Woerkom. Based on the corrected values, Sh G Sharaf and N A Budnikova recalculated the constants of integration and derived trigonometric formulas for the precession and tilt of the rotation axis, including terms of the second order for eccentricity and tilt. As a result, they calculated insolation variations for a period of 30 million years into the past and 1 million years into the future. Plots of equivalent latitudes by Sh G Sharaf and N A Budnikova are shown in Fig. 1. Equivalent latitudes for 65° north latitude are understood as latitudes at which the same amount of solar radiation is currently received during the summer caloric half-year as was received at parallel 65° north latitude in the past. An increase in the equivalent latitude means a reduction in the incoming

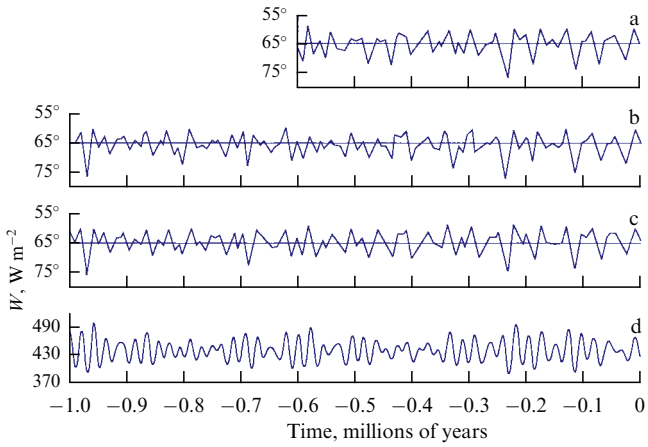

Figure 1. Changes in insolation over the summer caloric half-year for latitude 65° in the Northern Hemisphere according to data from various researchers [32]: (a) [6]; (b) [30]; (c) [31]; (d) [33]. Abscissa shows time in millennia from 1950, ordinate shows (a, b, c) insolation at equivalent latitudes during the summer half-year, (d) average monthly insolation in July W (W m^{-2}).

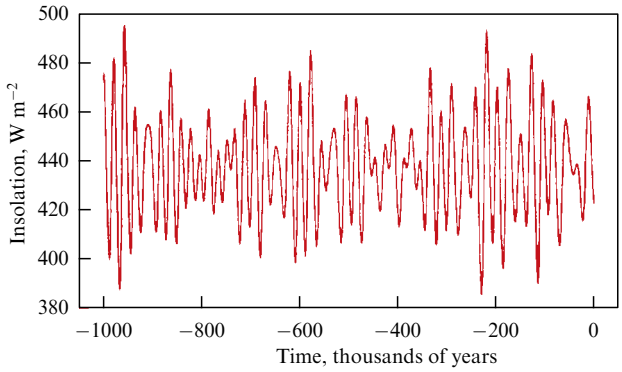

Figure 2. Insolation calculated for July 21 (120° geocentric longitude) for 65° N [34].

radiation and vice versa (for example, solar radiation coming to Earth at 65° N 590,000 years ago is typical for latitude 72° N in the epoch of 1800).

Jacques Laskar prepared a solution for the orbital, precession and tilt variables to calculate low-frequency variations in insolation [34]. He used astronomical ephemerides DE-406 (DE — Development Ephemerides) as a standard for testing his solutions in a short time period. Note that we used these DE-406 ephemerides as initial astronomical data for insolation calculations with high spatial and temporal resolution [35, 36]. In the cited paper [34], insolation was calculated only for the 65° north latitude parallel and only on one day of the year, when the Sun was at 120° of ecliptic longitude (summer in the Northern Hemisphere) with a step (at an interval of 1 million years) equal to 1000 years (see Fig. 2).

Using the values of the axis tilt angle, eccentricity, and perihelion longitude obtained by Sh G Sharaf and N A Budnikova, insolation values were calculated at the Institute of Oceanology of the Russian Academy of Sciences for a million years in the past and future relative to the present epoch (early 1950) with a time step of 5 thousand years and a latitude step of 10° [1, 3].

The total radiation for caloric half-years was calculated based on the relation

$$Q_{\mathrm{s,w}} = \frac{I_0 T_0}{2\pi}\left[S(\varphi,\varepsilon) \pm \sin\varphi\sin\varepsilon \pm \frac{4}{\pi} e \sin\Pi\cos\varphi\right], \quad (1)$$

where I_0 is the solar constant (equal to 2 cal min^{-1} cm^{-2} or 1395.6 W m^{-2}), T_0 is the tropical year duration (assumed constant), S is a function describing the annual distribution of insolation over a meridian, φ is the geographic latitude, Π is the perihelion longitude, e is the eccentricity, and ε is the ecliptic obliquity.

Recalculations of secular changes in the elements of Earth's orbit and insolation were also performed by A Vernekar [37]. Later, A Berger [38] proposed an improvement for the solution of D Brouwer and A Van Woerkom, including third-order terms for the eccentricity and tilt of the axis, and calculated the variations in the orbital elements and insolation. A comparison of the calculated solar radiation variations is shown in Fig. 1.

In general, the study of Earth's solar climate involves obtaining a series of calculated values of secular or low frequency variations of incoming solar radiation associated with secular variations in the elements of Earth's orbit: eccentricity, perihelion longitude, and tilt of the rotation axis. The quantitative results of this solution, calculations of secular variations in solar radiation, vary somewhat among different researchers due to differences in initial conditions and in methods of calculation (see Figs 1, 2).

Thus, several (at least 8) databases are currently known that reflect low-frequency variations in insolation, which can be included in the radiation block of physical and mathematical climate models [1, 6, 30, 31, 34, 37–39]. Insolation values or references to their location are indicated in the relevant publications. The data obtained by Anri Berger are used, for example, in the radiation block of the climate model of intermediate complexity at the Institute of Atmospheric Physics, Russian Academy of Sciences [40]. In addition, subprograms are known (for example, Daily INSOLation) that allow performing insolation calculations (for Earth and individual parallels) for a given time, taking into account changes in eccentricity, perihelion longitude, and axis tilt. Nevertheless, the CMIP recommendations do not take into account secular (or periodic) variations.

2.2.2 High-frequency (periodic) variations in irradiation. Calculations that take into account periodic perturbations of Earth's orbit, axis tilt, and associated high-frequency variations in solar radiation were performed at the Voeikov Main Geophysical Observatory (MGO) [41]. Currently, studies of high-frequency variations in insolation are being carried out at the Georges Lemaitre Institute of Astronomy and Geophysics (Belgium) [42–44]. However, calculations with a time resolution of one day were performed, first, for individual parallels, and second, only for four (points of equinoxes and solstices) or five (cardinal points and a point with a geocentric longitude of 120°) days in year. In our time, insolation calculations with high temporal resolution were performed by R G Cionco and W Soon 12 thousand years into the past (based on DE-431 ephemerides). They carried out calculations of insolation with a daily resolution, first, for individual parallels, and second, without taking into account the change in the duration of the tropical year [45]. That is, at present, for parameterization, there are four databases of

Earth's insolation, calculated taking into account periodic variations in solar radiation [41–45].

2.2.3 New insolation calculations and their differences from previous calculations. The mentioned insolation calculations (in the secular and periodic ranges) possess a number of disadvantages. To overcome them, the author, together with A A Kostin [35, 36], performed insolation calculations with high spatial and temporal resolution for 5000 years in the past and 999 years in the future (relative to the year 2000). Earth's insolation (irradiation energy — IE [J], specific irradiation energy — SIE [J m^{-2}], and irradiation intensity — II [W m^{-2}]) was calculated with a high spatial and temporary resolution. The calculations were performed using high-precision astronomical ephemerides (DE-406) [46, 47] for the upper boundary of the atmosphere (or Earth's surface without taking the atmosphere into account) in the interval from 3000 BCE to 2999 CE. The initial astronomical data for insolation calculations were the following: the declination and ecliptic longitude of the Sun, the distance from Earth to the Sun, and the difference in the course of the uniformly current coordinate time and the correctable universal time. Earth's surface was approximated by the Geodesic Reference System 1980 (GRS80) ellipsoid with semiaxes of 6378137 m (major) and 6356752 m (minor). In the general form, the calculation algorithm can be represented by the expression

$$I_{nm}(\varphi_1, \varphi_2) = \int_{t_1}^{t_2} \left(\int_{\varphi_1}^{\varphi_2} \sigma(\varphi) \left(\int_{-\pi}^{\pi} \Lambda(t, \varphi, \alpha)\, \mathrm{d}\alpha \right) \mathrm{d}\varphi \right) \mathrm{d}t\,, \quad (2)$$

where I is the incoming solar radiation for the elementary nth part of the mth tropical year [J]; σ is the area factor [m^2], used to calculate the area differential $\sigma(\varphi)\,\mathrm{d}\alpha\,\mathrm{d}\varphi$, i.e., the area of an infinitesimal trapezoid, a cell of the ellipsoid; α is the hour angle; φ_1, and φ_2 are geographic latitudes expressed in radians; $\Lambda(t, \varphi, \alpha)$ is the solar radiation at a given moment and a given point of the ellipsoid surface [W m^{-2}], and t is the time [s]. The integration steps were: in longitude 1°, in latitude 1°, and in time 1/360 of the tropical year duration, taking its change into account. Changes in solar activity were not taken into account. The value of the solar constant (average long-term TSI value) was taken equal to 1361 W m^{-2} [48]. The technique of calculating the solar energy that arrives at the Earth ellipsoid is described in detail in [13, 35, 36]. Variations in solar activity (TSI values based on the results of known reconstructions) are then easily taken into account in the calculated insolation data [49].

The main differences of our approach with respect to time, space, and initial data from the above-mentioned calculations of low-frequency variations in insolation are as follows.

1. *With respect to time*. M Milankovich and his followers calculated Earth's insolation for long periods of time (from several hundred thousand to millions of years) taking into account only its secular variations associated with changes in the eccentricity, perihelion longitude, and tilt of Earth's axis of rotation. The periods of change of these astronomical characteristics are several ten thousand years. The time resolution in the calculations was approximately from 5000 years in the calculations by M Milankovitch [6, 29], Sh Sharaf and N Budnikova [31], S A Monin [1] to 1000 years in the papers by A Vernekar [37], A Berger [33, 38], J Laskar [34]. Milankovich and his followers calculated daily and annual insolation for some initial year (for example, 1850 or 1950). Then a step was made from 1000 to 5000 years into the past or future, and the calculation procedure, taking into account changes in the eccentricity, longitude of the perihelion, and the axis tilt angle was repeated. Periodic variations in insolation were not taken into account. The duration of the tropical year was taken constant. Our calculations took into account the secular and periodic variations of such astronomical characteristics as the Earth–Sun distance, the tropical year duration, and the tilt angle of the rotation axis. The time resolution during integration in our calculations was 1/360 of the duration of a tropical year (approximately a day), taking into account variations in this duration [50].

2. *With respect to space*. M Milankovitch and all his followers performed calculations only for individual geographic parallels.Earth was considered a sphere. In our case, insolation is calculated for Earth's entire surface (approximated by an ellipsoid), hemispheres, and individual latitude zones. The spatial resolution in the course of integration was 1° in longitude and 1° in latitude. That is, in the calculations, M Milankovitch and his followers used a line, a first-order characteristic of space in mathematics. We calculated the insolation per area, a second-order spatial characteristic.

The influence of Earth's shape on the character of its irradiation was studied in [51]. To compare the irradiation of the ellipsoidal (with the present-day polar compression) and spherical Earth, the interval of tropical (astronomical) years from 3000 BCE to 2999 CE was chosen. The radius of the comparison sphere was chosen to ensure the same volume of the sphere and the ellipsoid. The insolation values were compared for the sphere and the ellipsoid on average for a year and for months of the year, then for hemispheres and semi-ellipsoids on average in half-years, then for 5-degree zones on average in half-years. That is, both temporal and spatial differences in the irradiation of the sphere and the ellipsoid were analyzed.

The insolation of the ellipsoid and the sphere on average for the year is 340.013 V m^{-2} and 340.302 W m^{-2}, respectively (the sphere irradiation is 0.085% higher than that of the ellipsoid). The average long-term monthly values of the irradiation intensity (II) of the ellipsoid and the sphere vary synchronously from the beginning to the end of the year. Minima are reached in the 3rd astronomical month (at aphelion), and maxima, in the 9th month (at perihelion). The difference between the long-term average monthly values of the sphere and ellipsoid irradiation in each month is positive. The annual behavior of this difference (Fig. 3) resembles the letter W with minima at the solstices and maxima at the equinoxes [51].

The latitude variations in the annual II for the sphere and the ellipsoid are small (Fig. 4).

The average annual II of the northern semi-ellipsoid and the Northern Hemisphere, respectively, are 419.818 W m^{-2} and 419.911 W m^{-2} in the first astronomical half-year and 257.334 W m^{-2} and 257.827 W m^{-2} in the second half-year. The average annual II of the southern semi-ellipsoid and the Southern Hemisphere, respectively, are 434.932 W m^{-2} and 435.028 W m^{-2} in the second astronomical half-year, and 248.392 W m^{-2} and 248.868 W m^{-2} in the first half-year. In each pair (semi-ellipsoid, hemisphere), the ratio of II in the warm half-year to II in the cold half-year is greater than the similar ratio for the hemisphere by 0.169%. In a series of differences in semi-annual insolation of the latitudinal zones of the sphere and the ellipsoid, the maximum is positive, and the minimum is negative. In the first astro-

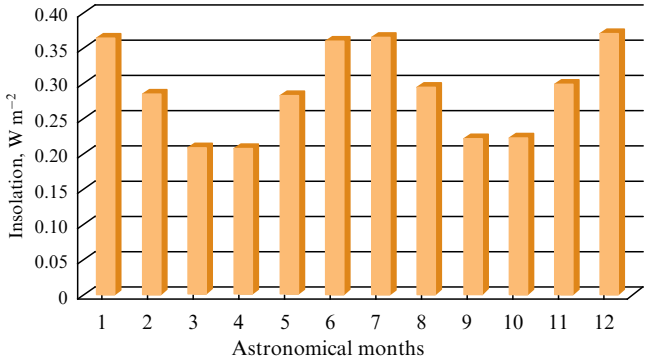

Figure 3. Difference between average multi-year monthly intensity of irradiation of the sphere and the ellipsoid.

nomical half-year, maximum II (0.0031 W m^{-2}) and minimum II (-0.0003 W m^{-2}) are observed in zones $45° - 50°$ S and $10° - 15°$ N, and in the second half of the year, in the zones $45° - 50°$ N (0.0032 W m^{-2}) and $10° - 15°$ S (-0.0003 W m^{-2}). It is worth noting that the spatial and temporary differences in the irradiation of the sphere and the ellipsoid are presented here for the average long-term values of insolation.

The modulus of the difference between the semi-annual II values for a semi-ellipsoid is greater than that for a hemisphere, by 0.247% for the northern pair or by 0.204% for the southern pair. The modulus of the difference between semi-annual values of II in the Northern (Southern) Hemisphere of Earth (seasonality of exposure, or insolation seasonality) is one of the key indicators of Earth's solar climate (Section 3.4.3) [7]. Thus, the average long-term insolation seasonality of Earth's Northern (Southern) Hemisphere for the ellipsoidal Earth is greater (due to the increase in surface curvature) than for the spherical Earth, by 0.247% (0.204%). Recall that seasonality in the solar climate of Earth is determined by the difference between the II of the summer and winter half-years.

For the interval from 1978 to 2008, it was shown in [51] that i) the average long-term modulus of the annual TSI anomaly is greater than the average long-term difference between the II for the sphere and the ellipsoid by 14.01%, and ii) the average long-term modulus of the monthly TSI anomaly exceeds the average long-term difference between the II for the sphere and the ellipsoid by 23.37%. This implies the conclusion that the differences (errors) in the calculation of the irradiation intensity of the sphere and the ellipsoid are commensurate with the TSI variations in the 11-year cycle that are currently noted.

3. To perform calculations for a long period, M Milankovitch calculated astronomical ephemerides for the eccentricity, perihelion longitude, and tilt of Earth's axis of rotation, which were further refined by his followers [30, 34, 37–39]. To calculate insolation, we used the parameters given in Eqn (2), which take into account the secular and periodic variations in the elements of Earth's orbit and the tilt of its rotation axis. The high-precision astronomical ephemerides DE-406 calculated at the Caltech Jet Propulsion Lab for the period from 3000 BCE to 2999 CE and available at the NASA electronic resource [47] were used as the initial data for the calculations.

The differences between our approach in calculating high-frequency (periodic) insolation variations and the methods of E P Borisenkov, M-F Loutre, C Bertrand, and their colleagues are associated, first, with the initial astronomical data used in the calculations, second, with different solutions to insolation calculations relative to Earth's surface, and third, with the time interval covered by the calculations. As initial data, E P Borisenkov and colleagues used ephemerides calculated at the Institute of Theoretical Astronomy of the Academy of Sciences of the USSR (e-mail message of A V Tsvetkov, 2015). The initial data for the calculations performed by Belgian researchers [43, 44] were the VSOP82 ephemerides [39]. In our calculations, we used the Jet Propulsion Laboratory (JPL) Planetary and Lunar Ephemerides DE-406 [46, 47].

When calculating insolation, the surface of Earth was identified by our predecessors with a sphere, and the calculations were performed only for individual parallels. E P Borisenkov et al. [41] obtained values only for parallels 20°, 40°, 60°, and 80° N. In the studies by Belgian researchers [44], calculations were performed (for mid-July, more precisely, for a point with a geocentric ecliptic longitude equal to 120°) only for the 65° parallel of northern latitude. For the equinoxes and solstices, insolation was calculated only for the equator and parallels of 30°, 60°, and 90° in each hemisphere.

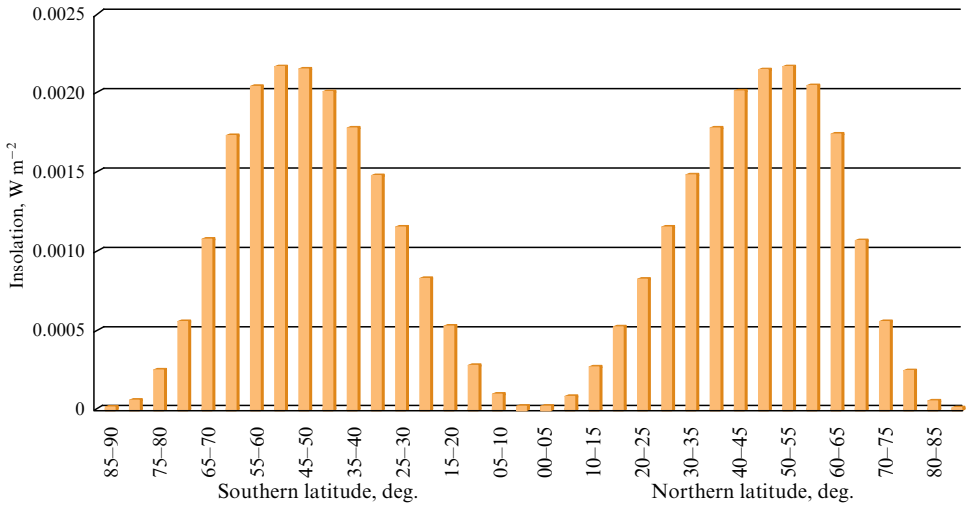

Figure 4. Difference between average long-term annual intensity of irradiation of the sphere and the ellipsoid in different latitudinal zones.

Recall that the geocentric longitude of the Sun is the angle between the directions from the center of Earth to the vernal equinox and the Sun. The points of the spring and autumn equinoxes are the points of intersection of the plane of Earth's orbit (ecliptic) with the plane of the celestial equator.

In the paper by C Bertrand et al. [43], insolation calculations cover the previous millennium; they also refer to June (a point with geocentric longitude equal to 120°) and are performed for the latitude zone of 65°–70° N. The values for the latitudinal zone were calculated by averaging the values obtained for its limiting parallels (65° and 70°). In our calculations, Earth's surface was approximated by an ellipsoid. The incoming radiation was calculated not for individual parallels but for the area of individual latitudinal zones with a latitude resolution of 1°, as well as for the area of hemispheres and the entire Earth. In addition, we obtained quantitative characteristics of the impact of Earth's shape on the nature of its surface irradiation (see Figs 3, 4) [51].

In the papers by E P Borisenkov et al., the time resolution in the calculations of high-frequency insolation variations approximately corresponds to a day [41]. However, their calculations are presented only for the winter and summer half-years and only for the Northern Hemisphere in the interval from 1800 to 2100. M-F Loutre et al. [44] performed calculations over an interval of 5000 years in the past with an annual resolution and only for July (a single point with a geocentric longitude of 120°), equinoxes, and solstices. In the paper by C Bertrand et al. [43], the insolation calculations cover the previous millennium, but they refer to only one month, July, and are performed with an annual resolution. In addition, the value of the solar constant in our calculations was taken equal to 1361 W m^{-2} [48]. Our predecessors used 1368 W m^{-2} [43], 1367 W m^{-2} in the paper by E P Borisenkov et al. [41] and M-F Loutre et al. [44], and 1366 W m^{-2} [42].

Our calculations are based on high-precision ephemerides. They use a new value of the solar constant (1361 W m^{-2}) [48] and cover a time interval of 5999 years and the entire surface of Earth in more detail. Earth in our calculations is not identified with a sphere, but is approximated by an ellipsoid. In this case, the difference in the calculated irradiation of a sphere and an ellipsoid of equal volume (which differ in surface curvature), as noted above, is commensurate with solar activity variations in the 11-year cycle (at present) [51]. The performed calculations, therefore, close the spatial and temporal 'gaps' in the calculations of insolation for the period from 3000 BCE to 2999 CE. This makes it possible to use the obtained insolation values in the radiation block of physical and mathematical climate models. The results obtained easily take into account the variations in solar radiation associated with the measurement of solar activity. To do this, it is enough to divide the available reconstructed TSI values by the value 1361 W m^{-2} used by us in the calculations, and then multiply the insolation values calculated by us by the obtained coefficients. Thus, variations of different physical natures are taken into account in changes in the total incoming solar radiation flow.

Based on the results of the calculations, a public database of incoming solar energy was formed in all latitudinal zones of the Earth ellipsoid (5 degrees wide) for each astronomical month of each year for the period from 3000 BCE to 2999 CE [52]. Earth insolation values are presented in data arrays in three units: J, J m^{-2}, and W m^{-2}. The dimensions correspond to the irradiation energy, specific irradiation energy, and irradiation intensity (which will be considered below) [51]. The values of incoming solar radiation calculated with high spatial and temporal resolution can be used in numerical experiments as an input external energy signal (incoming solar radiation) in the radiation block of physical and mathematical climate models.

Thus, there are opportunities to use Earth irradiation data as an input energy signal that varies over time with annual (as well as higher and lower) resolution. However, in a number of mathematical climate models, this possibility (taking into account secular or periodic variations in incoming solar radiation) remains unrealized. In this regard, such models with a simplified parameterization of solar radiation may have problems both at the stage of climate reproduction and at the stages of reconstructing or forecasting its changes.

3. Main problems of parameterization of the external radiative signal

Let us consider the problems of the radiation block using the example of well-known domestic physical and mathematical climate models of the Marchuk Institute of Numerical Mathematics of RAS (INM), the Obukhov Institute of Atmospheric Physics of RAS (IAP), and the Voeikov Main Geophysical Observatory (MGO). A joint model of the general circulation of the atmosphere and the ocean has been developed at the INM. This is the only Russian physical and mathematical model (INM Climate Model, INMCM) of climate participating in the CMIP project [18]. "The model includes the daily and seasonal variation of the Sun's height" ([53, p. 380]; [54, p. 228]). In other words, with the radiation block of this model, only diurnal and seasonal variations in solar radiation are currently taken into account, and its interannual and long-term (secular and periodic) changes are not taken into account. At the same time, as noted, there are real opportunities to consider them.

We can consider the atmospheric general circulation model, thoroughly described in the fundamental paper [55], the prototype of the AGCM (atmospheric general circulation model) in the INM RAS model. It declares that the basis of mathematical modeling of the general circulation of the atmosphere and ocean is a system of equations of hydrothermodynamics. As an energy source, it contains the term ε_r, which characterizes the radiative heating or cooling of air masses. Another characteristic of radiation processes in the atmosphere–Earth system is the amount of solar radiation absorbed by the surface layer of continents and oceans S_g and the downward flow of long-wave radiation near Earth's surface F_g (atmospheric counter-radiation). It is stated that "...the purpose of the radiation block in the general models of the atmosphere and ocean circulation is to determine the functions ε_r, S_g, F_g" ([55, p. 45]). In this case, to determine the functions ε_r, S_g, F_g in AGCM, the values of temperature, humidity, and pressure at the nodes of a three-dimensional finite-difference grid are used. All other parameters that determine the radiative process are either parameterized in terms of the indicated functions or are considered equal to some known average values [55]. Numerical experiments with the model were aimed at reproducing the main climatic characteristics. Forecasting was not considered at this stage. The atmospheric general circulation model (AGCM) was developed in the studies of V P Dymnikov, V N Lykosov, E M Volodin, et al. [56]. The basics of the ocean general circulation model (OGCM), a part of the INM joint model, are presented in papers by N A Dianskii [17, 54, 57]. The

incoming energy signal, without considering long-term (secular and periodic) and interannual variability, reflects the Keplerian unperturbed motion of Earth, which occurs in the absence of changes in the characteristics of its orbital motion (eccentricity, perihelion longitude, as well as periodic variations) and tilt of the rotation axis. Earth's actual motion is perturbed (Lagrangian), and the characteristics of Earth's orbital motion and the axis tilt, which determine its insolation (and the intensity of radiative heat transfer), change over time. Without considering long-term changes in irradiation for a certain geographical latitude at the same time (the same hour angle) on the same day (the same geocentric longitude of the Sun), the incoming energy signal in the IMV model will be equal to the same value after 10, 20, 100, or 1000 years. That is, the external energy signal (solar radiation) in the INM model depends on time only on the scale of the day and the seasons of the year and does not depend on time over longer intervals for which climatic characteristics are reconstructed or predicted. In connection with the simplified parameterization of solar radiation (disregard for long-term and interannual changes in the main energy signal, the radiation one), the reconstruction and forecasting of long-term climate changes seem to be very conditional. Taking into account the recommendations noted above (CMIP-5, CMIP-6), long-term variations in TSI can be taken into account in the model at the stage of reproducing climatic characteristics. However, first, they reflect variations in irradiation of only one physical nature associated with changes in the activity of the Sun. Variations associated with celestial-mechanical processes (except for the daily and annual variations) are not taken into account. Second, TSI data are available from reconstructions only for the past [19, 20, 23, 51] and from measurements for the present. Therefore, at the forecasting stage, it is not possible to take into account long-term changes in TSI realistically. In this regard, when modeling climate changes (both in the past and in the future), a number of problems arise that need to be solved, related to neglecting interannual and long-term (secular and periodic) variations in incoming solar radiation. Nevertheless, when discussing the difficulties existing in climate modeling, the problems associated with parameterization of solar radiation are not considered [15, 16, 58, 59]. In this regard, we should dwell on them in more detail.

3.1 Trends in long-term (secular) changes in incoming solar radiation

As shown by our calculations [60, 61] for the annual insolation of Earth (in this study, insolation is understood as the irradiation intensity II [W m^{-2}]) for the period covered by the calculations (from 3000 BCE to 2999 CE), a slow downward trend is notable, which amounts to 0.0055%. There is an increase in exposure in Earth's equatorial region (by 0.25%, relative to 3000 BCE) and a decrease in the polar regions (by 2.72%). That is, the modern era is characterized by an increase in the meridional contrast in the intensity distribution of Earth's annual II (Fig. 5).

The increase in meridional contrast is associated with a decrease in the angle of tilt of Earth's rotation axis. With a decrease in the axis tilt angle (relative to the perpendicular to the ecliptic plane), the arrival of solar radiation in the equatorial region increases and in the polar regions decreases. The result is an increase in insolation contrast and an increase in the meridional insolation gradient [6, 13].

The change in the semi-annual II has a different pattern of distribution over latitudes. In the first astronomical half-year, in the latitudinal region from 25° S to 90° N, II decreases (Fig. 6). The maximum reduction is 13.1 W m^{-2} (or 3.83%) and is observed in the polar zone of the Northern Hemisphere (85°–90° N). The increase in II in this half-year occurs in the latitude range of 25°–90° S. The value of II maximally increases by 1.97 W m^{-2} (1.96%) in the latitude zone of 55°–60° S.

In the second astronomical half-year in the latitudinal region of 50°–90° S, a reduction of II is noted. The maximum II reduction (by 6.05 W m^{-2}, or 1.71%) is typical for the polar zone of the Southern Hemisphere (85°–90° S). In the zone from 55° S to 90° N, II increases. The maximum increase in II (by 6.09 W m^{-2}, or 1.87%) falls in the latitudinal zone of 20°–25° N [13]. Thus, insolation seasonality is smoothed out in the Northern Hemisphere. In the Southern Hemisphere, the change in insolation seasonality over latitudes is more complex (see Fig. 6).

The latitudinal distribution of II in half-years (and seasons) is determined by the change in their duration associated with the angular relation of the line of nodes connecting the equinoctial points and the line of apsides connecting the aphelion and perihelion of Earth's orbit [13].

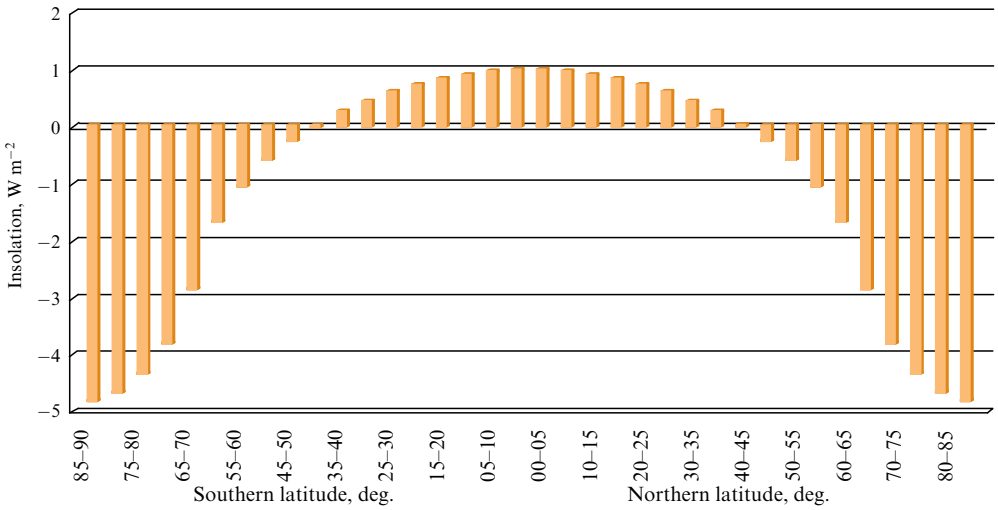

Figure 5. Secular change in annual intensity of Earth irradiation in interval from 3000 BCE to 2999 CE.

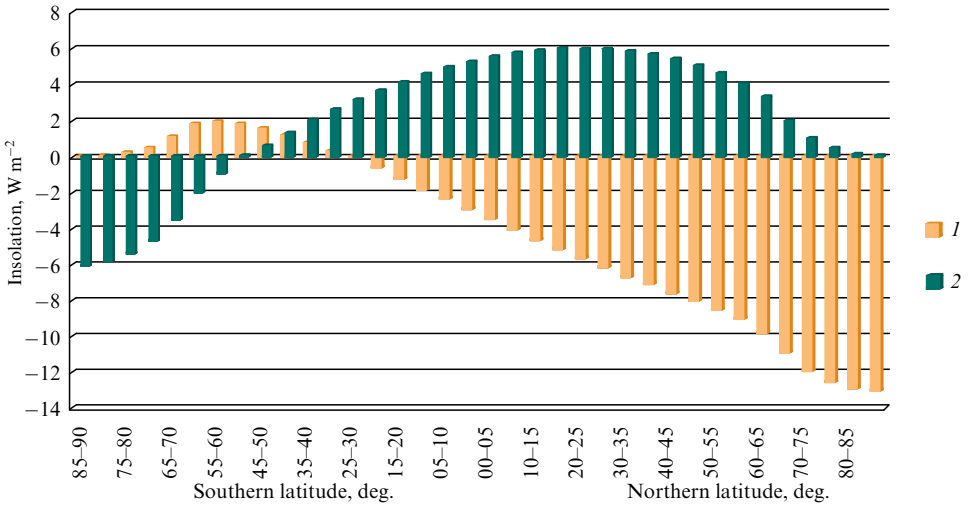

Figure 6. Secular change in intensity of irradiation of Earth in first (*1*) and second (*2*) astronomical half-years versus latitude.

This ratio changes due to the precession of the vernal equinox and the movement of the perihelion of Earth's orbit.

3.2 Periodic variations in solar radiation

Periodic variations are characteristic of most hydrometeorological processes. However, the radiation block of climate models (INM, MGO, etc.) currently does not allow for periodic variations in insolation [53, 54, 59], which can be the cause of periodic variations in hydrometeorological characteristics. Earth's real motion is perturbed. Due to periodic changes in the orbital characteristics (above all, the Earth-to-Sun distance, tropical year duration) and axial tilt (nutation), periodic variations in the irradiation of Earth occur (Fig. 7) [62].

Against the background of the above secular trends in Earth's irradiation, 19-year variations complicating it have been noted (Figs 7, 8). Such a periodicity in Earth's insolation was also noted by our predecessors, who performed calculations in the range of high-frequency insolation variations [4, 43–45, 63]. In the 19-year periodicity, cycles lasting 8 and 11 years are distinguished, which, in turn, are formed by two- and three-year cycles ($2+3+3=8$-year cycle and $2+3+3+3=11$-year cycle). At the same time, the irradiation of Earth from an eight-year cycle to an 11-year cycle in a 19-year nutation periodicity changes (Fig. 8), either strengthening or weakening the abovementioned trend of increasing meridional contrast. The amplitude of II variations in the 19-year cycle in the polar regions is about 0.07% of the solar radiation coming to these regions. It is known that TSI variations taken into account (in accordance with the CMIP recommendations) in physical and mathematical climate models also amount to 0.07% in an 11-year cycle [64, 65].

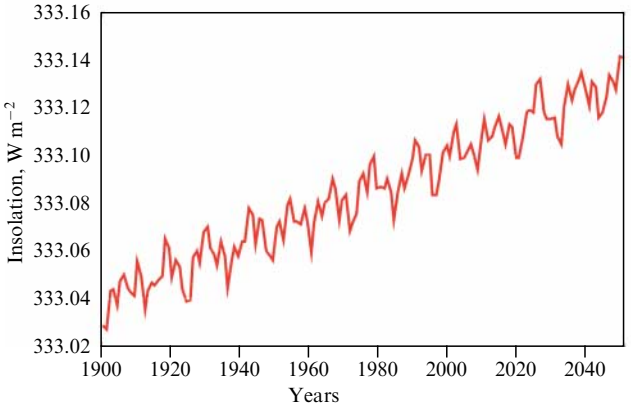

Figure 7. Long-term periodic changes in Earth II in the first astronomical half-year in the interval from 1900 to 2050.

The noted two- and three-year periodicity is associated with commensurability in the average motions of Earth with the nearest planets — Mars and Venus [13, 50]. It is known that a number of interesting relationships are observed in the motion parameters of planets and their satellites due to the presence of commensurability and resonances [66, 67]. The resonance conditions are determined by the equality of the frequencies of induced (under the action of an external force) and natural oscillations. Let us consider this issue in more detail. The sidereal, or stellar, period of a planet's revolution is the period of time during which the planet makes one complete revolution around the Sun in its orbit. The sidereal period of Venus is 224.701 days (0.61521 tropical year), of Mars is 686.980 days (1.88089 tropical year), and of Earth (sidereal year) is 365.526 days (1.00004 tropical years). The rotational frequencies of the planets ($\omega = 2\pi/T$) are 0.0279624 day^{-1} for Venus, 0.0091460 day^{-1} for Mars, and 0.0171894 day^{-1} for Earth. This implies $2\omega_{\text{Mars}}$ (0.0182920 day^{-1}) $-\omega_{\text{Earth}}$ (0.0171894 day^{-1}) $=$ 0.0011026 day^{-1} and $3\omega_{\text{Venus}}$ (0.0838872 day^{-1}) $-5\omega_{\text{Earth}}$ (0.085947 day^{-1}) $=$ $-$ 0.0020598 day^{-1}. This result indicates that in the orbital motions of Earth and the nearest planets Mars and Venus there is a commensurability (the form of connection of orbital objects): the orbital resonance is 2/1 for Earth with Mars and 3/5 for Earth with Venus [66–68].

Thus, every two terrestrial years, the mutual positions of Earth with Mars and every three years of Earth with Venus relative to the Sun are repeated. These repetitions are associated with periodic perturbations of Earth's orbital motion (Earth–Sun distance, tropical year duration) and, consequently, variations in solar radiation arriving at Earth during a tropical year (see Fig. 7). The proportion of the two- and three-year cycles in the series of interannual II changes reflects the relative perturbing action of the nearest planets. About 70% of the cycles of the studied time series (of

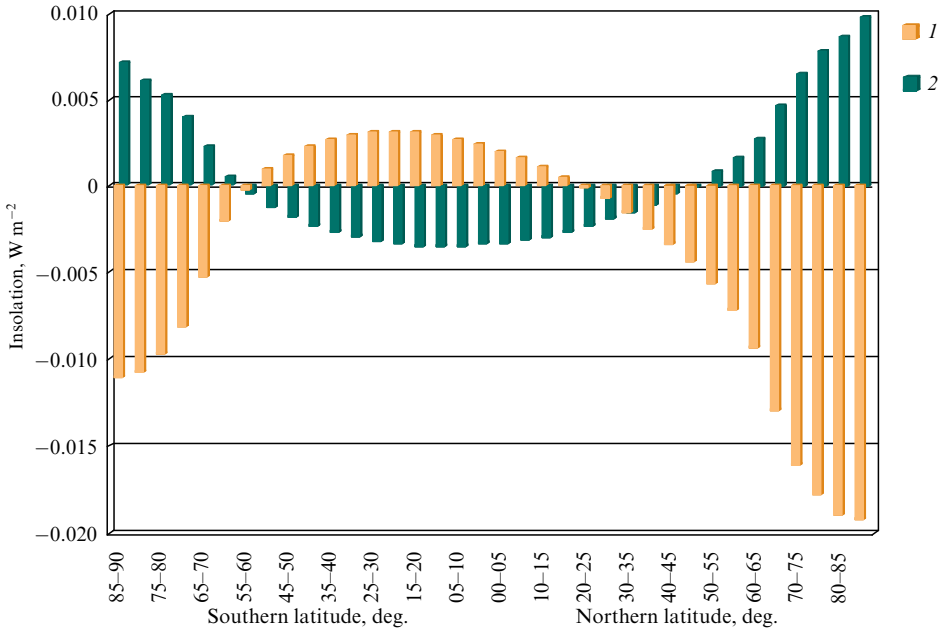

Figure 8. Latitudinal changes in Earth's insolation (II) in the 19-year nutation cycle (*1* — in the 2000–2010 phase, *2* — in the 2011–2019 phase).

arbitrary duration) are formed by three-year cycles, which are determined by perturbations of Earth's orbital motion by Venus. The rest of the time series, about 30%, is represented by two-year cycles, which are determined by a weaker perturbation of Earth's orbital motion by Mars [69]. Due to the noted proportion of two- and three-year cycles in spectral analysis, the maximum spectral density falls on oscillations with a period of 2.7 years (which do not exist in reality) [13, 50, 65]. It is this statistical peak that was noted by all our predecessors as dominant in the spectral analysis of periodic insolation changes [41, 43–45, 63]. A peak with a period of 2.7 years is also noted in the spectral analysis of individual climatic characteristics [70]. Integer periodicity in insolation and many natural processes is associated with Earth's annual revolution around the Sun and its commensurability with the orbital motions of the Moon and the nearest planets Venus and Mars (and Jupiter, resonance 1/12). The above two- and three-year variations in II can be related to the quasi-biennial and quasi-triennial oscillations (QBOs and QTOs) known in the variability of climatic characteristics [71].

Long-term periodic variations in the irradiation of the hemispheres and individual latitudinal zones during astronomical seasons and months have an even greater amplitude than the periodic variations in the Earth irradiation [13]. As a result of the periodic perturbing action of the Moon, the Sun and the planets, Earth has an osculating orbit. That is, it is permanently moving along an ellipse, but at each moment of its movement, it is a new ellipse. Because of the perturbed motion, every year Earth comes to the vernal equinox sometimes earlier, sometimes later, and every year at a different distance from the Sun, as a result of which Earth's orbital motion forms a torus with a diameter of about 30 thousand km [72, 73].

The variations mentioned above can be amplified by the resonant response of Earth's natural system and its components for a perturbation multiple of the year (the system's proper period). In addition, the effect of stochastic resonance is possible, i.e., the response of a bistable system to a weak periodic signal under exposure to noise of a certain power [74–77]. The noted fluctuations in insolation can be considered a weak periodic signal for Earth's natural system under noise exposure. In the case of resonance, the amplitude of fluctuations of hydrometeorological characteristics dependent on solar radiation can increase many times (causing an extreme event). Such a resonance is possible with a small external multiply repeated impact on the system [74].

Considerable attention is devoted by the authors of the INM model to the assessment of possible climate changes under small external impacts, i.e., the problem of climate sensitivity [15, 78, 79]. Nevertheless, the small periodic variations in solar radiation, the main source of energy, are not included in the radiation block of this model (nor in other models). At the same time, already in the first energy-balance models [80, 81], "the instability of snow and ice cover with respect to small fluctuations in insolation" was shown ([82, p. 268]). At the same time, a close connection between changes in sea ice area and surface air temperature and ocean surface temperature was obtained [83]. This dependence is also characterized by the presence of positive feedback [80]. The noted relationship between periodic changes in climatic characteristics and periodic changes in insolation confirms the need for parameterization of small periodic (other than the annual cycle included in the radiation blocks of all models) insolation variations in the mathematical modeling of climate.

In the well-known astronomical theory of climate, secular variations in solar radiation are calculated in connection with secular perturbations of two orbital elements, the orbital eccentricity and perihelion longitude, as well as the tilt angle of the rotation axis. At the same time, it is believed that "perturbations are of two kinds: periodic, occurring within extremely narrow limits, and secular. The former have almost no effect on the irradiation of the Earth and therefore are of no interest to us" ([6, p. 37]). This statement is true only when considering climatic changes on geological time scales with a coarse discreteness in time. In such cases, a time resolution of 1 to 5 thousand years is used in insolation calculations, which filters periodic variations out [1, 6, 30, 31, 33, 34, 37, 39].

However, generally erroneous ideas about the insignificant effect of periodic (small) variations of II on climate change are also projected onto its current changes (on the scale of decades and centuries). As noted above, the annual exposure in the period from 3000 years ago to 2999 in the polar zones decreased by 4.82 W m^{-2} (see Fig. 5). Consequently, on average per year, the secular change in II in this zone amounted to 0.0008 W m^{-2}. At the same time, as follows from Fig. 8, periodic II change in the nutation cycle in 2000–2011 in the northern polar zone reaches approximately 0.02 W m^{-2}. The annual average change in II in this case is 0.0018 W m^{-2}. In the first astronomical half-year in the northern polar zone, the secular reduction II is equal to 13.09 W m^{-2} (see Fig. 6). On average, summer insolation in the polar zone of the Northern Hemisphere for 5999 years decreases by 0.0022 W m^{-2} per year. Thus, on a real-time scale, periodic and secular variations in insolation are quite commensurate in magnitude. This also confirms the need to take into account in the radiation block both secular and periodic variations in the Earth irradiation occurring simultaneously.

3.3 Interannual variability of solar radiation

Seasonal changes in climatic characteristics are known to be closely related to the annual variation in incoming solar radiation (determined by the tilt angle of the rotation axis). The long-term variations in surface air temperature (SAT) and ocean surface temperature (OST), as will be shown in Section 3.4.1, are closely related to insolation contrast (determined by the change in the tilt angle of the rotation axis). The interannual variability of climatic characteristics is determined by natural fluctuations in the global system and its components. Such fluctuations are mainly stochastic, and therefore they are particularly difficult to model and forecast. However, at the same time, spatial and temporal features are noted, indicating the presence of regularities in the interannual variability of the characteristics of the natural environment state. For example, for the Arctic Ocean, a close relationship was found between the annual behavior of the mean modulus of interannual variability of the sea ice area and the annual course of irradiation in the Northern Hemisphere, shifted by 2 months into the past [84].

Techniques based on the Markov properties of natural variability are successfully used to study interannual climate variability. Such a technique, in particular, was successfully tested in the study of the natural variability of climate characteristics in the northern polar region of the Northern Hemisphere [85]. Regular features were also found in the interannual variability of insolation. It exhibits, for example, periodic oscillations (see Section 3.2) for the irradiation intensity. There are cycles of 8 and 11 years duration (constituting a 19-year nutation cycle or Metonic cycle in total), which, in turn, are formed by two- and three-year cycles ($2 + 3 + 3 = 8$-year cycle and $2 + 3 + 3 + 3 = 11$-year cycle). Recall that the Metonic cycle is associated with the approximate equality of 19 tropical years to 235 synodic months (i.e., every 19 years the lunar cycle ends on the same day of the solar year). This cycle reflects the phase inequality in the perturbing effect of the Moon on Earth's orbital motion and the nature of its irradiation. The nutation cycle reflects the tropical inequality of tides or the perturbing effect of the Moon on Earth's rotation axis [65, 69].

Climate models (e.g., INM, MGO, IAP) currently do not take into account the interannual variability of solar radiation. In summer seasons in the polar regions (for which the greatest discrepancies are observed in model calculations both between individual models and between model and real values of climatic characteristics [86]), the average interannual variability of the irradiation intensity (over the studied time interval) in absolute value is 0.011 W m^{-2}, or 0.043%, in the Northern Hemisphere and 0.010 W m^{-2}, or 0.042% (of the average II for a latitudinal zone), in the Southern Hemisphere (Fig. 9). If we take into account that the amplitude of TSI variations in the 11-year cycle (about 1 W m^{-2}) is 0.07% (from 1361 W m^{-2}), then the value of the interannual TSI variability in the cycle will be approximately equal to 0.024–0.037%. Consequently, the interannual variability of insolation (II) commensurate with the interannual variability of TSI can also be recommended to be

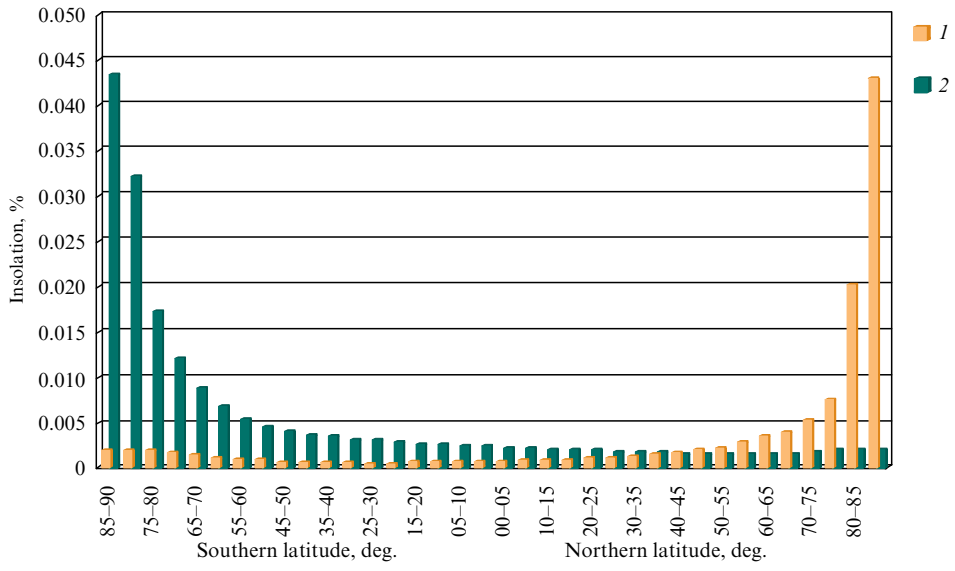

Figure 9. Latitude distribution of the modulus of average interannual changes in intensity of the irradiation of Earth in the first (*1*) and second (*2*) astronomical half-year.

taken into account in the radiation block of physical and mathematical climate models [13, 64, 65].

Thus, the radiation block of the INM and MGO models currently does not consider secular and periodic variations in II, despite the possibility of taking them into account based on available insolation data and/or using existing computational routines for secular oscillations [53, 54]. The radiation block of the models does not take into account interannual changes in insolation either. The simplified content of the radiation block of physical and mathematical models and the lack of using the available opportunities to supplement it can decrease the adequacy and realism of model constructions. Therefore, secular and periodic variations, as well as interannual variability of solar radiation coming to Earth, must be taken into account in the parameterization of the radiation block of climate models.

3.4 Mechanisms of radiative heat transfer

The main mechanisms of radiative heat transfer in the ocean–atmosphere system are meridional heat transfer (''heat engine of the first kind''), heat transfer in the ocean–continent system (''heat engine of the second kind''), and interhemispheric heat transfer [10, 11]. Models (INM, MGO, etc.) currently take into account only the average annual values of meridional energy (heat) transfer in the atmosphere and ocean and do not take into account long-term (secular and periodic) changes in the intensity of radiative heat transfer.

3.4.1 Meridional transfer of radiative heat. Due to the nonuniform distribution of solar radiation over Earth's surface, a meridional insolation gradient (MIG) associated with the shape of Earth arises [87–90]. MIG, as noted above, increases with a decrease in the tilt of the rotation axis (this is observed at present) and decreases with an increase in the tilt angle. Based on the performed calculations, a latitudinal profile of the change in the annual MIG over 5999 years at the UBA was obtained (Fig. 10). The maxima of the MIG increase are localized near the polar circles (latitude 60°–70°, the annual zones of geophysical instability). By the zones of instability, we mean the latitudinal zones in which the maximum changes in the MIG are detected when its sign changes. These zones of instability coincide with the areas of maximum development of extratropical cyclones (cyclogenesis) in the hemispheres. In addition, an increase in the annual values of MIG also occurs in the areas of localization of the Hadley and Ferrel circulation cells in the atmosphere, while a decrease is noted in the areas of localization of polar cells [13].

Figure 11 shows long-term changes in MIG for the winter and summer (in the Northern Hemisphere) half-year. The value of the seasonal MIG increases to the maximum in the winter (for the Northern Hemisphere or in the second astronomical) half-year in the latitudinal zone of 15°–20° S (11.8%) and decreases to the maximum in the zone of 10°–15° S (−17.8%). In the summer (for the Northern Hemisphere or the first astronomical) half-year, the maximum increase (11.8%) is noted in the latitudinal zone of 10°–15° N, and the maximum reduction (−17.8%) is noted in the latitudinal zone of 5°–10° N.

As follows from Fig. 11, in the summer half-years in both hemispheres, seasonal (summer) instability zones are distinguished, located in the range of 5°–20° of latitude. Here, in the neighboring five-degree latitudinal zones, maximum discrepancies are noted in the trends of the summer MIG changes. Summer zones of instability in the transfer of radiative heat coincide with the areas of generation of tropical cyclones localized in the latitude ranges of 5°–20° of each hemisphere [91]. The operation of a 'heat engine of the first kind' is associated with the vortex energy transfer — the mechanism of meridional heat transfer (MHT) from low latitudes to high latitudes [87–90]. In the polar regions (polar circulation cells), in the winter half-years of the hemispheres, an increase in seasonal MIG is noted, as is a decrease in the summer half-years.

The distribution of average values for latitudinal zones (over the period from 3000 BCE to 2999 CE) of the annual MIG was compared with the latitudinal distribution of the average annual energy transfer in the ocean–atmosphere system used in models [92, 93]. At the same time, the numerical values of energy transfer in the ocean–atmosphere system in [92, 93] are on average 6–7 times higher than the MIG values, which is associated with the participation of water and air masses in the energy transfer in the ocean–

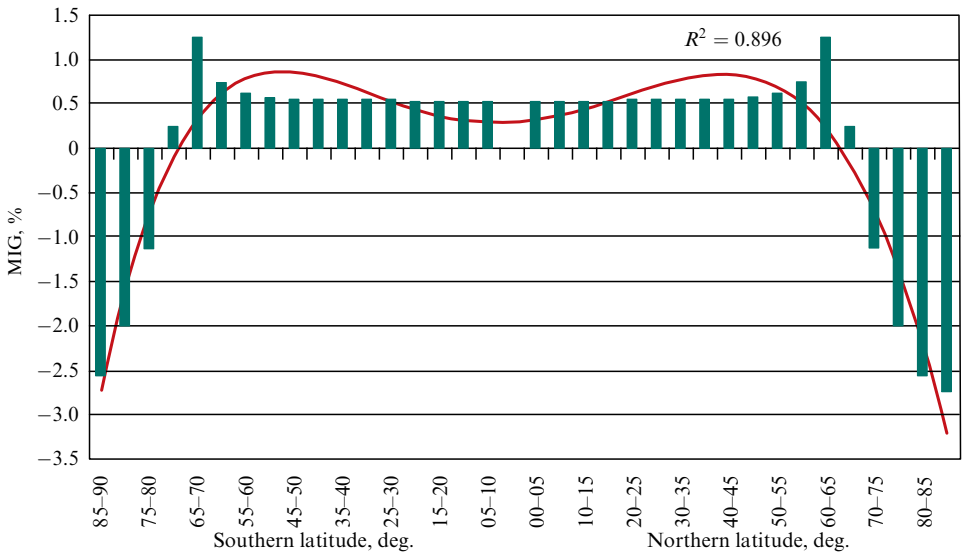

Figure 10. Change in annual MIG in latitude zones for 5999 years (approximation by a fourth-order polynomial) in percent with respect to 3000 BCE.

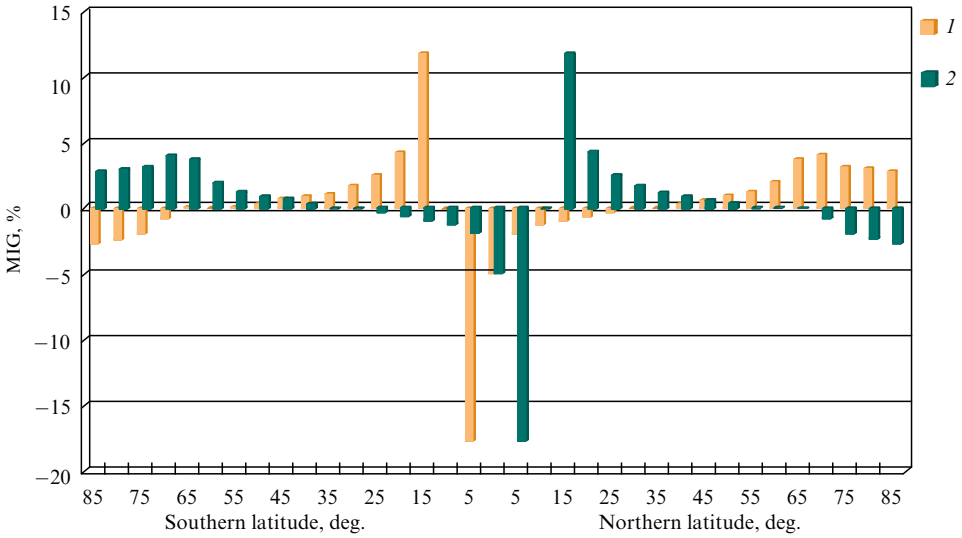

Figure 11. Seasonal MIG change in latitudinal zones over 5999 years as a percentage of 3000 BCE (*1* — winter, *2* — summer half-year for the Northern Hemisphere).

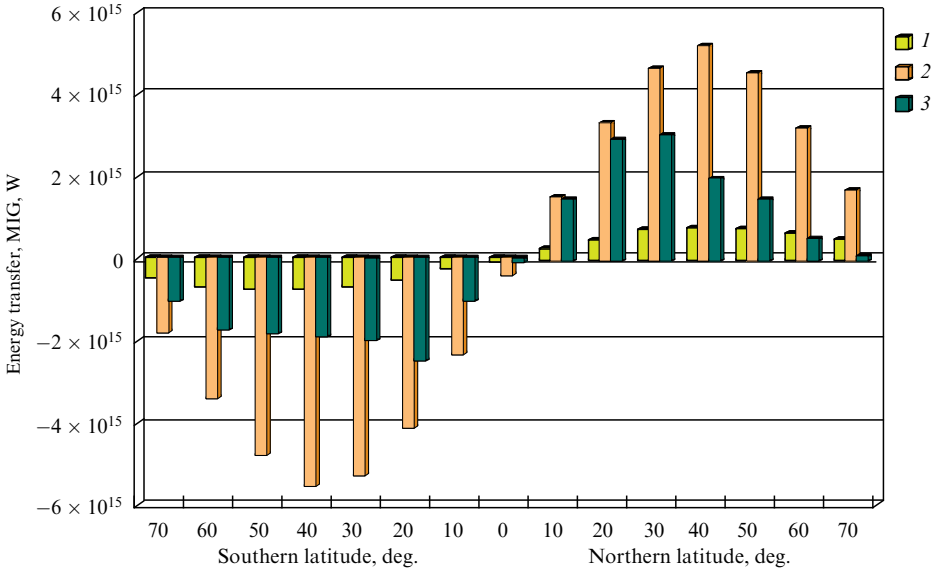

Figure 12. Average long-term value of the annual MIG *1* and the average annual energy transfer in the ocean–atmosphere system in latitudinal zones: *2* — according to [92], *3* — according to [93].

atmosphere system (Fig. 12). In other studies, the energy transfer values are approximately 3–5 times higher than the annual MIG values [94, 95]. The value of the correlation coefficient between the latitudinal distributions of MIG and the latitudinal distribution of energy transfer in the ocean–atmosphere system varies from 0.981 [92] to 0.895 [93].

Since the energy transfer in the ocean–atmosphere system is determined by MIG (the inverse is impossible), the features found for it can manifest themselves in the ocean–atmosphere system (an increase or decrease in the circulation intensity in the atmosphere general circulation cells and in the ocean, in the intensity of the meridional eddy energy transfer, and, therefore, in climatic variability). A change in the intensity of meridional transport (in the ocean and atmosphere) affects the thermal regime, smoothing out meridional temperature differences in the hemispheres. In this case, it should be borne in mind that the area from which the radiative heat comes (heat source) is approximately 2.7 times more than the area of the heat sink areas. Therefore, the change in temperature with a change in the intensity of radiative heat transfer manifests itself most noticeably at high latitudes [89, 96–98].

We took the annual insolation contrast as a characteristic of the meridional transfer of radiative heat. The insolation contrast (IC) reflects MIG, summarized by the areas of heat source and sink. Long-term changes in the annual IC are linearly related to long-term changes in the tilt angle of the rotation axis (negative relationship). For the hemispheres, the annual IC was calculated from the obtained insolation values as the difference between solar radiation arriving at the latitudinal region of 0°–45° (heat source) and 45°–90° (heat sink) per year. Changes in OST and SAT of Earth and hemispheres (data from the University of East Anglia and the Met Office Hadley for the period from 1900 to 2016) are mainly taken into account by trends [13, 14]. The value of the determination coefficient is from 0.693 to 0.862 (the trends are polynomials of the second degree). The determination

Table. Long-term changes in SAT and SST explained by the regression model [14, 97, 98].

Factors	Earth/World Ocean	Northern Hemisphere	Southern Hemisphere
Surface air temperature (SAT)			
IC	80.7 %	73.4 %	83.1 %
IC and AMO	88.3 %	86.4 %	84.0 %
Ocean surface temperature (OST)			
IC	79.7 %	69.3 %	84.1 %
IC and AMO	88.5 %	86.6 %	85.9 %
Note: Atlantic Multidecadal Oscillation (AMO) is a climatic oscillation with a period of about 60 years.			

coefficient shows the proportion of changes in OST and SAT, determined by the trend. Therefore, in order to explain the trends in long-term changes in global temperature, it is necessary to identify the factor that determines the trends in the initial OST and SAT series. Analyses show that long-term changes in the OST and SAT of Earth and the hemispheres are characterized by close positive correlations with long-term changes in IC and negative correlations with long-term changes in the tilt angle of the axis. Recall that the change in climatic season (or temperature) during the year is due to the fact that the axis of rotation of Earth has a tilt. Therefore, the relationship between the trend in global temperature change and the change in this tilt angle of Earth's axis of rotation seems reasonable and natural. Calculations performed using regression equations (based on an ensemble of linear and polynomial solutions) showed that long-term changes in SAT and OST by more than 2/3 are determined by long-term changes in insolation contrast (Table).

As noted, long-term changes in IC are linearly related to changes in the tilt angle of the axis, which decreased from 1900 to 2016 by 0.015°. IC has increased during this time by 0.7 W m^{-2}. SAT and OST rose by approximately 1 °C and 0.9 °C, respectively.

The physical mechanism of the close relationship found between long-term changes in global temperature (SAT and OST) and insolation contrast can be summarized as follows. Associated with a decrease in the tilt angle, an increase in IC, which regulates the meridional transfer of radiative heat or the intensity of the 'heat engine of the first kind,' leads to an increase in heat transfer by circulation processes and vortex formations in the atmosphere from low latitudes to high ones. As noted, the area of annual regions of heat sources is approximately 2.7 times more than the area of annual heat sink regions in the hemispheres. Consequently, the energy transferred from low to high latitudes is distributed over a smaller area and its specific characteristics increase. As a result of meridional heat transfer, SAT and OST increase in areas of its sink (apparent heat). This leads to an increase in evaporation, an increase in the content of water vapor in the atmosphere, and an intensification of the greenhouse effect. As a result, there is an additional influx of heat and an increase in temperature, etc. Such a process, repeating many times, forms a mechanism for increasing climate warming. In addition, because of condensation due to the advection of warm air masses from low to high latitudes, latent heat is released, which makes an additional contribution to the scheme of radiative heat transfer in the atmosphere. Positive feedback should also be taken into account — a decrease in albedo due to a decrease in the area of sea ice and mountain glaciers, as well as the duration of snow cover. As a result, the surface (continents and oceans) heats up more and the atmosphere heats up from it. It should be noted that, due to differences in the hemispheres (the Northern Hemisphere is more continental and less homogeneous than the Southern Hemisphere), climate change in them is somewhat different. First of all, there are more eddy formations (tropical and extratropical cyclones) in the Northern Hemisphere than in the Southern Hemisphere, in which the underlying surface is more homogeneous. Annually in the Northern Hemisphere there are from 60 to 70 tropical cyclones, and only 5–10 in the Southern Hemisphere. Second, in the Southern Hemisphere, the meridional heat transfer is noticeably blocked by zonal circulation, the 'Roaring Forties' in the atmosphere, and the Antarctic Circumpolar Current in the ocean. Therefore, the warming processes are more noticeable in the Northern Hemisphere [13, 14, 97, 98]. Thus, the described physical mechanism can explain the observed features in the change in the modern global climate: warming and increasing its instability (increase in the frequency of extreme event occurrence [99]), associated with the activation of eddy processes (tropical and extratropical cyclones).

The current increase in ocean surface temperature [100, 101] implies a decrease in CO_2 solubility. As the climate cools, the solubility of CO_2 in cooling seawater increases, which (given the stability of CO_2 sources) should lead to a decrease in its partial pressure (content) in the atmosphere. Simultaneous measurements of carbon dioxide content in the atmosphere and sea water show that the content of CO_2 in water is basically close to some equilibrium value corresponding to the content of CO_2 in the air, but changes with a decrease or increase in water temperature, respectively, upward or downward [12, 102]. Considering that the world's oceans occupy about 71% of Earth's area, such a decrease in CO_2 solubility with an increase in ocean surface temperature and salinity can significantly affect the increase in atmospheric CO_2. The conclusion that the main factor determining the fluctuations in the content of CO_2 in the atmosphere should be considered the variation in the exchange of carbon dioxide in the ocean and atmosphere due to a change in the temperature of ocean waters was made back in the 20th century by I V Altunin and E P Borisenkov [103] and confirmed by B M Smirnov [12] in the 21st century based on studies carried out. Carbon dioxide is probably not a cause [104, 105], but a consequence [13, 14, 28, 97, 106, 107] of climate change. The change in OST and SAT is currently mainly determined by the insolation contrast (IC) and the Atlantic Multidecadal Oscillation (AMO) [108–110] (see Table).

The meridional energy transfer in the first models of the general circulation of the atmosphere was calculated taking into account the mean latitudinal distribution of the radiation

balance [111]. The equations of hydro-thermodynamics used in modern models of the general circulation of the atmosphere (AGCM) and the ocean (OGCM) also take into account the average value of the annual meridional energy (heat) transfer in the ocean–atmosphere system (see Fig. 12) and do not take into account the changes in the annual and seasonal MIG. At the same time, as shown by simple regression models, the trends in SAT and OST changes are closely related to changes in IC, which are generalized by areas of heat source and sink reflecting changes in MIG (see Table).

3.4.2 Interhemispheric transfer of radiative heat. Let us consider one more mechanism of radiative heat transfer to UBA, interhemispheric heat transfer. Interhemispheric heat exchange in the atmosphere is regulated by the insolation seasonality of Earth (ISE), which (like the climatic precession cycle) is determined by the ratio of precession and perihelion longitude cycles. ISE is characterized by the difference between the insolation seasonality in the Northern (Southern) Hemisphere and the insolation seasonality in the Southern (Northern) Hemisphere. Estimates of the air mass transported in the atmosphere were obtained by N S Sidorenkov (for 1970–1974). On average, during these five years, about 4×10^{18} g of air was transported from the summer hemisphere to the winter hemisphere [11]. Interhemispheric exchange thus supplied about 0.08% of the atmosphere mass. However, the transfer of radiative heat (by air and water masses) from the summer hemisphere to the winter one changes with time due to the difference between summer and winter insolation in the hemispheres. Because of interhemispheric transfer of radiative heat, one winter hemisphere can receive more or less heat than another winter hemisphere. For example, the small (medieval) climatic optimum of the Holocene is associated with the maximum interhemispheric transfer of radiative heat at UBA (transfer to the winter Northern Hemisphere from the summer Southern Hemisphere) (Fig. 13) [49].

The interhemispheric transfer of radiative heat at the upper boundary of the atmosphere was calculated as follows. We calculated 1) the difference between summer insolation (irradiation intensity, [W m^{-2}]) in the Southern Hemisphere and winter insolation in the Northern Hemisphere, 2) the difference between summer insolation in the Northern Hemisphere and winter insolation in the Southern Hemisphere. By subtracting one difference from the other, a function was obtained that reflects the total annual transfer of radiative heat from one hemisphere to the other [W m^{-2}]. In this case, when subtracting the difference 2 from the difference 1, positive values correspond to the predominance of the annual transport from the summer Southern Hemisphere to the winter Northern Hemisphere, and negative values, on the contrary, to the predominance of the transport from the summer Northern Hemisphere to the winter Southern one.

When comparing the differences, it turns out that the interhemispheric transfer of radiative heat (at the UBA) from the summer Southern Hemisphere to the winter Northern Hemisphere exceeds the transfer of heat from the summer Northern Hemisphere to the winter Southern Hemisphere (at the calculated interval). At the same time, the maximum in the differences in the interhemispheric transfer of radiative heat falls in the years 850–1000 (see Fig. 13) [49]. The value of difference in interhemispheric radiative heat transfer in

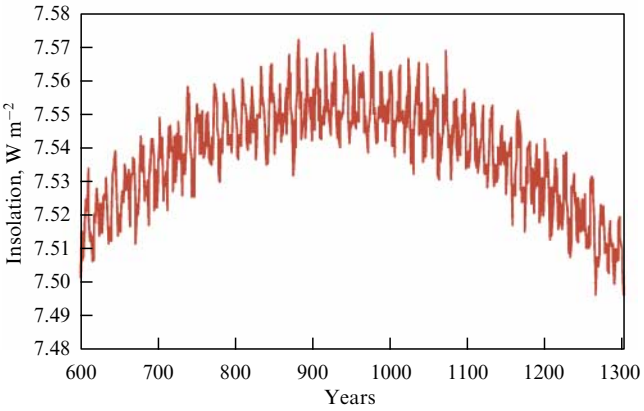

Figure 13. Maximum interhemispheric transfer of radiative heat (in the Northern Hemisphere).

3000 BCE is 2.59 W m^{-2}. In the maxima (years 881, 940, 976), it is about 7.57 W m^{-2}. That is, an increase from the value of 3000 BCE to the maximum, which falls within the period of years from 850 to 1000, is about 5 W m^{-2}. The mechanism of interhemispheric heat transfer in the atmosphere is realized through the Hadley circulation cell of the winter hemisphere partially shifted to the summer hemisphere. We present the transfer from 1 m^2 of the surface of the hemisphere. To estimate the total transport intensity for the hemisphere, the obtained values should be multiplied by the area of the hemisphere ($2.550328025 \times 10^{14}$ m^2). For the maximum in 976, this value will be 1.9232×10^{15} W, which is comparable to the annual MIG and energy transfer in the ocean–atmosphere system (see Fig. 12). Considering that the meridional annual energy transfer in the ocean–atmosphere system is 3–7 times greater than the annual MIG (Section 3.4.1) and assuming that this ratio is preserved in the interhemispheric transfer, one can estimate the interhemispheric energy transfer in the ocean– atmosphere system. In this case, for the ISE maximum of 976, the interhemispheric energy transfer in the ocean–atmosphere system can range from 5.76961×10^{15} W to 1.34624×10^{16} W.

It should be noted that variations associated with solar activity (TSI) do not manifest themselves in interhemispheric heat transfer. This is determined by the fact that, during the astronomical half-year (in general, any interval of a tropical year), the variations associated with the activity of the Sun are the same in the hemispheres. The presented new data on the direction and intensity of radiative heat transfer can also be taken into account in the radiation block of climate models.

3.4.3 Radiative heat transfer in the ocean–continent system. Heat exchange in the ocean–continent system, a ''heat engine of the second kind,'' is determined by the insolation seasonality of the hemisphere (ISH), which is also regulated by the ratio of the precession cycle (preceding the equinoxes) and the perihelion longitude cycle (with a period of about 22 thousand years). Insolation seasonality of the hemisphere is calculated as the difference between summer and winter insolation in the hemisphere (it is assumed that Earth has the shape of an ellipsoid (Section 2.2.3)) [7]. Long-term changes in the intensity of heat transfer in the ocean-continent system are associated with seasonal changes in the heat source and sink areas. When seasonal differences in insolation are smoothed out, the intensity of heat transfer in the ocean–

continent system decreases and seasonal temperature differences increase. Conversely, with an increase in insolation seasonality, the intensity of heat transfer in the ocean–continent system increases and seasonal temperature differences smooth out. For the period from 3000 BCE to 2999 CE, insolation seasonality in the Northern Hemisphere increases by 12.1 W m^{-2}, or by 7.1% (seasonal temperature differences are smoothed out). In the Southern Hemisphere during the same period, insolation seasonality decreases by 2.3 W m^{-2}, or by 1.3%, and the temperature seasonal differences increase [14]. This is because, in the time interval under consideration, Earth passes through perihelion, when it is winter in the Northern Hemisphere, and aphelion, when it is summer in the Northern Hemisphere. Thus, seasonal differences in the irradiation intensity (II) in the Northern Hemisphere are smoothed out in the modern era. In the Southern Hemisphere, summer occurs at the perihelion of Earth's orbit, winter, at aphelion, and seasonal differences of II in this hemisphere increase.

The above mechanisms of radiative heat transfer enhance or weaken the latitudinal temperature contrast (meridional transfer) and seasonal temperature differences (interhemispheric transfer, transfer in the continent–ocean system) in the atmosphere. Fluctuations in the inflow of solar radiation and in the transfer of radiative heat are determined by secular and periodic changes in the characteristics of Earth's orbital motion and the tilt angle of Earth's rotation axis, i.e., the features of its orbital and rotational motions.

Long-term changes in the intensity of radiative heat transfer should be taken into account in the radiation block of physical and mathematical climate models for a more complete and realistic reflection of the state of the natural system and the processes occurring in it both in the present and in the future. The results of calculations of long-term changes in solar radiation are available in [35, 41, 43–45]. However, at present, if even modeling takes the heat transfer into account, then only on average (for example, the meridional heat transfer in the energy transfer equation. This reduces the quality of climate reproduction and the reliability of forecasting its changes.

4. Conclusion

The radiation block is an obligatory element of physical and mathematical climate models. As a rule, it takes into account the values of the daily and annual behavior of irradiation, as well as instrumental and reconstructed solar activity data. Some models take into account secular changes in incoming radiation. With such a parameterization of the initial radiation data, the models do not take into account long-term (periodic) and inter-annual changes in Earth's irradiation, or long-term changes in the intensity of radiative heat transfer. The realism and reliability of the results of modeling the state of a nonlinear oscillatory natural system depend on the completeness and accuracy of the initial radiation data, since solar radiation is the main source of energy for the processes occurring in it (hydrometeorological, geochemical, etc.). When modeling nonlinear processes in a natural system, the reliability of reproduction and the depth of the forecast are reduced due to the increase in errors and uncertainties associated with insufficient completeness and accuracy of the initial radiation data.

Currently, periodic and interannual changes in exposure, as well as long-term changes in the intensity of radiative heat transfer, are not taken into account in the radiation block of climate models, which are based on the ideology of N A Phillips, S Manabe, and J Smagorinsky, embedded in climate modeling (with the priority task of developing a general atmospheric circulation model based on hydrodynamic equations) more than half a century ago, when calculations of the irradiation of Earth with high spatial and temporal resolution had not yet been performed.

Solving the problems associated with limitations in the radiation block parameterization is possible based on taking into account the radiation data (Earth's solar climate) obtained by calculation methods, reflecting the secular and periodic variations in the incoming radiation and the intensity of radiative heat transfer at the UBA. Taking into account in a deeper volume and refining the initial conditions of the main external energy signal can facilitate an increase in the reliability of physical and mathematical climate models and forecasts of its changes.

This study was carried out in accordance with the state budget themes Paleographic Reconstruction of Natural Geosystems and Forecasting their Changes (no. 121051100135-0) and Evolution of, Current State of, and Forecast for the Development of the Coastal Zone of the Russian Arctic (no. 121051100167-1).

References

1. Monin A S *An Introduction to the Theory of Climate* (Dordrecht: D. Reidel Publ. Co., 1986); Translated from Russian: *Vvedenie v Teoriyu Klimata* (Leningrad: Gidrometeoizdat, 1982)
2. Kondrat'ev K Ya *Global'nyi Klimat i Ego Izmeneniya* (Global Climate and Its Changes) (Leningrad: Nauka, 1987)
3. Monin A S, Shishkov Yu A *Phys. Usp.* **43** 381 (2000); *Usp. Fiz. Nauk* **170** 419 (2000)
4. Budyko M I *Izv. Akad. Nauk SSSR. Ser. Geograf.* (5) 36 (1968)
5. Kondrat'ev K Ya *Changes in Global Climate: a Study of the Effect of Radiation and Other Factors During the Present Century* (Rotterdam: A.A. Balkema, 1985); Translated from Russian: *Radiatsionnye Faktory Sovremennykh Izmenenii Global'nogo Klimata* (Leningrad: Gidrometeoizdat, 1980)
6. Milankovitch M *Mathematische Klimalehre und astronomische Theorie der Klimaschwankungen* (Handbuch der Klimatologie, Bd. 1. Allgemeine Klimalehre, Hrsg. W Koppen, R Geiger) (Berlin: Borntraeger, 1930); Translated into Russian: *Matematicheskaya Klimatologiya i Astronomicheskaya Teoriya Kolebanii Klimata* (Mathematical Climatology and Astronomical Theory of Climate Fluctuations) (Moscow–Leningrad: GONTI, 1939); *Mathematische Klimalehre und astronomische Theorie der Klimaschwankungen* (Nendeln, Liechtenstein: Kraus Reprint, 1972)
7. Monin A S, Shishkov Yu A *Istoriya Klimata* (History of Climate) (Leningrad: Gidrometeoizdat, 1989)
8. Drozdov O A et al. *Klimatologiya* (Climatology) (Leningrad: Gidrometeoizdat, 1989)
9. Khromov S P, Petrosyants M A *Meteorologiya i Klimatologiya* (Meteorology and Climatology) (Moscow: Izd. MGU, 2006)
10. Shuleikin V V *Fizika Morya* (Sea Physics) (Moscow: Izd. AN SSSR, 1953)
11. Sidorenkov N S *Atmosfernye Protsessy i Vrashchenie Zemli* (Atmospheric Processes and the Earth Rotation) (St. Petersburg: Gidrometeoizdat, 2002)
12. Smirnov B M *Fizika Global'noi Atmosfery. Parnikovyi Effekt, Atmosfernoe Elektrichestvo, Izmenenie Klimata* (Physics of the Global Atmosphere. Greenhouse Effect, Atmospheric Electricity, Climate Change) (Dolgoprudnyy: Intellekt, 2017)
13. Fedorov V M *Insolyatsiya Zemli i Sovremennye Izmeneniya Klimata* (Earth Insolation and Modern Climate Change) (Moscow: Fizmatlit, 2018)
14. Fedorov V M *Gidrometeorolog. Ekologiya* (64) 435 (2021)

15. Dymnikov V P, Lykosov V N, Volodin E M *Izv. Atmos. Ocean. Phys.* **42** 568 (2006); *Izv. Ross. Akad. Nauk Fiz. Atmos. Okeana* **42** 618 (2006)
16. Dymnikov V P, Lykosov V N, Volodin E M *Herald Russ. Acad. Sci.* **82** 111 (2012); *Vestn. Ross. Akad. Nauk* **82** 227 (2012)
17. Lykosov V N et al. *Superkomp'yuternoe Modelirovanie v Fizike Klimaticheskoi Sistemy* (Supercomputer Modeling in the Physics of the Climate System) (Moscow: Izd. Moskovskogo Univ., 2012)
18. Dymnikov V P, Lykosov V N, Volodin E M *Izv. Atmos. Ocean. Phys.* **51** 227 (2015); *Izv. Ross. Akad. Nauk Fiz. Atmos. Okeana* **51** 260 (2015)
19. Lean J, Beer J, Bradley R *Geophys. Res. Lett.* **22** 3195 (1995)
20. Lean J et al. *Solar Phys.* **230** 27 (2005)
21. CMIP5 recommendations. Recommendations for CMIP5 solar forcing data. SOLARISHEPPA, http://solarisheppa.geomar.de/cmip5
22. CMIP6 recommendations. Recommendations for CMIP6 solar forcing data. SOLARISHEPPA, https://solarisheppa.geomar.de/cmip6
23. Steinhilber F et al. *Proc. Natl. Acad. Sci. USA* **109** 5967 (2012)
24. Eigenson M S *Solntse, Pogoda i Klimat* (Sun, Weather and Climate) (Leningrad: Gidrometeoizdat, 1963)
25. Dergachev V A, Raspopov O M *Solnechno-Zemnaya Fiz.* (12-2) 272 (2008)
26. Zherebtsov G A et al. *Cosmic Res.* **46** 358 (2008); *Kosmich. Issled.* **46** 4368 (2008)
27. Eliseev A V, Mokhov I I *Fundament. Priklad. Klimatolog.* **1** 119 (2015)
28. Connolly R et al. *Res. Astron. Astrophys.* **21** (6) 131 (2021)
29. Milankovitch M *Théorie Mathématique des Phénomènes Thermiques produits par la Radiation Solaire* (Paris: Gauthier-Villarset et Cie, 1920)
30. Brouwer D, Van Woerkom A J, in *Astronomical Papers Prepared for the Use of the American Ephemeris and Nautical Almanac* Vol. 13, Pt. 2 (Washington, DC: U.S. Govt. Print. Off., 1950) p. 81
31. Sharaf Sh G, Budnikova N A *Trudy Inst. Teoret. Astron. Akad. Nauk SSSR* (14) 48 (1969)
32. Mel'nikov V P, Smul'skii I I *Astronomicheskaya Teoriya Lednikovykh Periodov*: *Novye Priblizheniya. Reshennye i Nereshennye Problemy* (Astronomical Theory of Ice Ages: New Approximations, Solved and Unsolved Problems) (Novosibirsk: GEO, 2009)
33. Berger A, Loutre M F *Quat. Sci. Rev.* **10** 297 (1991)
34. Laskar J, Joutel F, Boudin F *Astron. Astrophys.* **270** 522 (1993)
35. Fedorov V M, Kostin A A *Protsessy Geosredakh* (2) 254 (2019)
36. Fedorov V M, Kostin A A, in *Processes in GeoMedia* Vol. 1 (Springer Geology, Ed. T O Chaplina) (Cham: Springer, 2020) p. 181, https://doi.org/10.1007/978-3-030-38177-6_20
37. Vernekar A D, in *Long-Period Global Variations of Incoming Solar Radiation* (Meteorological Monographs, Vol. 12, No. 34) (Boston, MA: American Meteorological Society, 1972)
38. Berger A L *J. Atmos. Sci.* **35** 2362 (1978)
39. Bretagnon P *Astron. Astrophys.* **114** 278 (1982)
40. Mokhov I I, Eliseev A V, Guryanov V V *Dokl. Earth Sci.* **490** 23 (2020); *Dokl. Ross. Akad. Nauk* **490** (1) 27 (2020)
41. Borisenkov Ye P, Tsvetkov A V, Agaponov S V *Climatic Change* **5** 237 (1983)
42. Berger A, Loutre M-F, Yin Q *Quat. Sci. Rev.* **29** 1968 (2010)
43. Bertrand C, Loutre M F, Berger A *Geophys. Res. Lett.* **29** (18) 40 (2002)
44. Loutre M-F et al. *Climate Dyn.* **7** 181 (1992)
45. Cionco R G, Soon W W-H *Earth-Sci. Rev.* **166** 206 (2017)
46. Standish E M "JPL Planetary and Lunar Ephemerides", DE405/LE405. Interoffice memorandum: JPL IOM 312.F-98-048, 1998, August 26
47. Solar System Dynamics. Jet Propulsion Laboratory. California Institute of Technology. National Aeronautics and Space Administration, https://ssd.jpl.nasa.gov
48. Kopp G, Lean J L *Geophys. Res. Lett.* **38** L01706 (2011)
49. Fedorov V M et al. *Izv. Atmos. Ocean. Phys.* **57** 1239 (2021); *Geofiz. Protsessy Biosfera* **20** (3) 5 (2021)
50. Fedorov V M *Dokl. Earth Sci.* **451** 750 (2013); *Dokl. Ross. Akad. Nauk* **451** (1) 95 (2013)
51. Fedorov V M, Kostin A A, Frolov D M *Izv. Atmos. Ocean. Phys.* **56** 1301 (2020); *Geofiz. Protsessy Biosfera* **19** (3) 119 (2020)
52. Solar Radiation and Climate of the Earth. Solar Climate Theory. Solnechnaya Radiatsiya i Klimat Zemli. Solyarnaya Teoriya Klimata, http://www.solar-climate.com/
53. Galin V Ya *Izv. Atmos. Ocean. Phys.* **34** 339 (1998); *Izv. Ross. Akad. Nauk Fiz. Atmos. Okeana* **34** 380 (1998)
54. Dianskii N A *Modelirovanie Tsirkulyatsii Okeana i Issledovanie Ego Reaktsii na Korotkoperiodnye i Dolgoperiodnye Atmosfernye Vozdeistviya* (Modeling Ocean Circulation and Studying Its Response to Short- and Long-Term Atmospheric Forcing) (Moscow: Fizmatlit, 2013)
55. Marchuk G I et al. *Matematicheskoe Modelirovanie Obshchei Tsirkulyatsii Atmosfery i Okeana* (Mathematical Modeling of the General Circulation of the Atmosphere and Ocean) (Leningrad: Gidrometeoizdat, 1984)
56. Volodin E M et al. *Izv. Atmos. Ocean. Phys.* **53** 142 (2017); *Izv. Ross. Akad. Nauk Fiz. Atmos. Okeana* **53** (2) 164 (2017)
57. Volodin E M, Diansky N A *Izv. Atmos. Ocean. Phys.* **42** 267 (2006); *Izv. Ross. Akad. Nauk Fiz. Atm. Okeana* **42** (3) 291 (2006)
58. Simmons A J, Bengtsson L "Atmospheric general circulation models: their design and use for climate studies", in *The Global Climate* (Ed. J T Houghton) (Cambridge: Cambridge Univ. Press, 1984); Translated into Russian: in *Global'nyi Klimat* (Ed. J T Houghton) (Leningrad: Gidrometeoizdat, 1987) p. 94
59. Shneerov B E et al. *Trudy Glavnoi Geofiz. Observ. im. A I Voeikova* (550) 3 (2001)
60. Fedorov V M *Phys. Usp.* **62** 32 (2019); *Usp. Fiz. Nauk* **189** 33 (2019)
61. Fedorov V M, Frolov D M *Cosmic Res.* **57** (3) 156 (2019); *Kosmich. Issled.* **57** (3) 177 (2019)
62. Fedorov V M *Dokl. Earth Sci.* **457** 869 (2014); *Dokl. Ross. Akad. Nauk* **456** 2222 (2014)
63. Borisenkov Ye P, Tsvetkov A V, Eddy J A *J. Atmos. Sci.* **42** 933 (1985)
64. Makarova E A, Kharitonov A V, Kazachevskaya T V *Potok Solnechnogo Izlucheniya* (Solar Radiation Flux) (Moscow: Nauka, 1991)
65. Fedorov V M *Solar System Res.* **46** 170 (2012); *Astron. Vestn.* **46** 184 (2012)
66. Grebenikov E A, Ryabov Yu A *Rezonansy i Malye Znamenateli v Nebesnoi Mekhanike* (Resonances and Small Denominators in Celestial Mechanics) (Moscow: Nauka, 1978)
67. Roy A E *Orbital Motion* (New York: Wiley, 1978); Translated into Russian: *Dvizhenie po Orbitam* (Moscow: Mir, 1981)
68. Beletsky V V *Essays on the Motion of Celestial Bodies* (Basel: Birkhäuser Verlag, 2001); Translated from Russian: *Ocherki o Dvizhenii Kosmicheskikh Tel* (Moscow: Nauka, 1972)
69. Fedorov V M *Gravitatsionnye Faktory i Astronomicheskaya Khronologiya Geosfernykh Protsessov* (Gravitational Factors and Astronomical Chronology of Geospheric Processes) (Moscow: Izd. Mosk. Univ., 2000)
70. Ivanov V V *Phys. Usp.* **45** 719 (2002); *Usp. Fiz. Nauk* **172** 777 (2002)
71. Kulyamin D V, Dymnikov V P *Izv. Atmos. Ocean. Phys.* **46** 432 (2010); *Izv. Ross. Akad. Nauk Fiz. Atmos. Okeana* **46** 467 (2010)
72. Duboshin G N *Nebesnaya Mekhanika. Analiticheskie i Kachestvennye Metody* (Celestial Mechanics. Analytical and Qualitative Methods) (Moscow: Nauka, 1978) p. 456
73. Fedorov V M *Solar System Res.* **50** 220 (2016); *Astron. Vestn.* **50** 233 (2016)
74. Blekhman I I *Sinkhronizatsiya Dinamicheskikh Sistem* (Synchronization of Dynamical Systems) (Moscow: Nauka, 1971)
75. Anishchenko V S et al. *Phys. Usp.* **42** 7 (1999); *Usp. Fiz. Nauk* **169** 7 (1999)
76. Anishchenko V S, Anufrieva M V, Vadivasova T E *Tech. Phys. Lett.* **32** 873 (2006); *Pis'ma Zh. Tekh. Fiz.* **32** (20) 12 (2006)
77. Anishchenko V S et al. *Nonlinear Dynamics of Chaotic and Stochastic Systems*: *Tutorial and Modern Developments* (Berlin: Springer, 2002)
78. Dymnikov V P et al. *Sibirsk. Zh. Vychislit. Matem.* **6** 347 (2003)
79. Dymnikov V P et al. *Russ. Meteorol. Hydrol.* (4) 53 (2004); *Meteorolog. Gidrolog.* (4) 77 (2004)
80. Budyko M I *Tellus* **21** 611 (1969)
81. Sellers W D *J. Appl. Meteorol. Climatol.* **8** 392 (1969)

82. Untersteiner N "The cryosphere", in *The Global Climate* (Ed. J T Houghton) (Cambridge: Cambridge Univ. Press, 1984); Translated into Russian: in *Global'nyi Klimat* (Ed. J T Houghton) (Leningrad: Gidrometeoizdat, 1987) p. 259
83. Wôlsh J E, Chapman W L *Ann. Glaciology* **33** 444 (2001)
84. Fedorov V M, Grebennikov P B *Earth's Cryosphere* **25** (2) 35 (2021); *Kriosfera Zemli* **25** (2) 38 (2021)
85. Alekseev G V, Svyashchennikov P N *Estestvennaya Izmenchivost' Kharakteristik Klimata Severnoi Polyarnoi Oblasti i Severnogo Polushariya* (Natural Variability of Climate Characteristics in the Northern Polar Region and the Northern Hemisphere) (Leningrad: Gidrometeoizdat, 1991)
86. Sherstyukov B G *Regional'nye i Sezonnye Zakonomernosti Izmenenii Sovremennogo Klimata* (Regional and Seasonal Regularities of Changes in Modern Climate) (Obninsk: VNIIGMI-MTsD, 2008)
87. Davis B A S, Brewer S *Climate Dyn.* **32** 143 (2009)
88. Soon W, Legates D R *J. Atmos. Solar-Terr. Phys.* **93** 45 (2013)
89. Fedorov V M *Izv. Atmos. Ocean. Phys.* **55** 1572 (2019); *Geofiz. Protsessy Biosfera* **18** (3) 117 (2019)
90. Cionco R G, Soon W W-H, Quaranta N E *Adv. Space Res.* **66** 720 (2020)
91. Khromov S P *Meteorologiya i Klimatologiya dlya Geograficheskikh Fakul'tetov* (Meteorology and Climatology for Geographical Departments) (Leningrad: Gidrometeoizdat, 1968) p. 492
92. Lorenz E N *The Nature and Theory of the General Circulation of the Atmosphere* (Geneva: World Meteorological Organization, 1967); Translated into Russian: *Priroda i Teoriya Obshchei Tsirkulyatsii Atmosfery* (Leningrad: Gidrometeoizdat, 1970)
93. Palmén E, Newton C W *Atmospheric Circulation Systems*: *Their Structure and Physical Interpretation* (New York: Academic Press, 1969); Translated into Russian: *Tsirkulyatsionnye Sistemy Atmosfery* (Leningrad: Gidrometeoizdat, 1973)
94. Peixóto J P, Oort A H *Rev. Mod. Phys.* **56** 365 (1984)
95. Trenberth K E, Caron J M *J. Climate* **14** 3433 (2001)
96. Woods J D "The upper ocean and air-sea interaction in global climate", in *The Global Climate* (Ed. J T Houghton) (Cambridge: Cambridge Univ. Press, 1984); Translated into Russian: *Global'nyi Klimat* (Ed. J T Houghton) (Leningrad: Gidrometeoizdat, 1987) p. 298
97. Fedorov V M *Georisk* **14** (4) 16 (2020)
98. Fedorov V M *Geomagn. Aeronomy* **62** 932 (2022)
99. Ruzmaikin A *Phys. Usp.* **57** 280 (2014); *Usp. Fiz. Nauk* **184** 297 (2014)
100. Lee K et al. *Nature* **396** 155 (1998)
101. Huang B, Liu Z *J. Climate* **14** 3738 (2001)
102. Golubev V N *Kriosfera Zemli* **14** (4) 17 (2010)
103. Altunin I V, Borisenkov E P *Dokl. Akad. Nauk SSSR* **316** 3574 (1991)
104. Byalko A V *Phys. Usp.* **55** 103 (2012); *Usp. Fiz. Nauk* **182** 111 (2012)
105. The Intergovernmental Panel on Climate Change, IPCC, https://www.ipcc.ch/
106. Monin A S, Berestov A A *Herald Russ. Acad. Sci.* **75** 52 (2005); *Vestn. Ross. Akad. Nauk* **75** 126 (2005)
107. Kondrat'ev K Ya, Demirchyan K S *Herald Russ. Acad. Sci.* **71** 623 (2001); *Vestn. Ross. Akad. Nauk* **71** 1002 (2001)
108. Schlesinger M E, Ramankutty N *Nature* **367** 723 (1994)
109. Sutton R T, Hodson D L R *Science* **309** 115 (2005)
110. Chylek P, Lesins G *J. Geophys. Res.* **113** D22106 (2008)
111. Manabe S, Smagorinsky J, Strickler R F *Mon. Weather Rev.* **93** 769 (1965); Translated into Russian: in *Teoriya Klimata* (Collection of translated articles, Eds L S Gandin, A S Dubov, M E Shvets) (Leningrad: Gidrometeoizdat, 1967) p. 185